Eur. Phys. J. E **23**, 367–374 (2007)
DOI 10.1140/epje/i2006-10198-5

THE EUROPEAN PHYSICAL JOURNAL E

Domain-induced budding in buckling membranes

A. Minami[a] and K. Yamada

Department of physics, Kyoto University, Kyoto 606-8502, Japan

Received 12 December 2006 and Received in final form 2 May 2007
Published online: 22 August 2007 –

Abstract. We present a phase field model on buckling membranes to analyze phase separation and budding on soft membranes. By numerically integrating dynamic equations, it turns out that the formation of caps is greatly influenced by the presence of a little excess area due to the surface area constraint. When cap-shaped domains are created, domain coalescence is mainly observed not between domains with same budding directions, but between domains with opposite budding directions, because the bending energy between two domains is larger in the former case. Although we do not introduce spontaneous curvature like Helfrich model, we obtain some suggestions related to the slow dynamics of the phase separation on vesicles.

PACS. 82.45.Mp Thin layers, films, monolayers, membranes – 87.16.Dg Membranes, bilayers, and vesicles

1 Introduction

It is well known that biomembranes are composed mainly of phospholipids and cholesterol and have characteristic heterogeneities due to the immiscibility of them. Simons *et al.* suggested that these heterogeneities play an important roles in the activity of the biomembranes [1]. After this model, termed raft model, was suggested, vesicles composed of saturated lipids, unsaturated lipids and cholesterol have attracted attention as a minimal model of the raft model, and a number of studies have been carried out experimentally [2–9] and theoretically [10–19]. For example in phase separations on the soft membranes, the geometry of the membrane and the phase separation are coupled via line tensions of domain boundaries [20] or curvature differences between components [12,13]. In the presence of positive surface tensions of membranes, due to the competition between the curvature difference and the surface tension, hexagonal and stripe pattern formation on the membrane is reported [6,21–23].

In particular, vesicles have often become an attracting topic of physical and biological researches. Recently, Yanagisawa *et al.* [9] reported the phase separations on vesicles with excess area. In their systems, the domain coarsening is suppressed at a certain domain size in the presence of the surface excess area. They attributed this slow dynamics to the repulsive inter-domain interactions originating from the membrane elasticity. In the presence of the surface excess area, cap-shaped domains are created. There is a large bending energy between two caps as they get closer, and the inter-domain interaction becomes repulsive. However, there is no reasonable theoretical explanation of this effect. Here, in this paper, we interpret the excess area in another way.

To avoid complexity, let the membrane be flat. In membranes, there are two elastic modes — off-plane mode and in-plane mode. The off-plane and the in-plane modes are, respectively, corresponding to a deformation perpendicular and parallel to the membrane. Usually, the in-plane deformation is energetically very hard compared to the off-plane deformation in so-called soft membranes. If we apply in-plane compression to such membranes, the area applied by this deformation escapes in the off-plane direction due to the high incompressibility. This is called buckling instability, and this area applied by the deformation can be interpreted as the excess area. Therefore, we focus on the phase separation on the buckling membranes to understand the budding and the coarsening on membranes. Even if the slow dynamics of the phase separation on vesicles is not reproduced by our approach, the buckling of soft membranes might be an interesting operation experimentally and theoretically.

2 Model equations

To evaluate the interaction energy between phase boundaries and deformation of membranes correctly, we introduce the differential geometry on deformed membranes. Strictly speaking, we should evaluate every derivatives by the metric tensor $g_{\alpha\beta}$. However, to avoid complexity, we focus attention on the minimal mathematical structure to describe domain-induced budding on buckling membranes, and derive dynamic equations.

[a] e-mail: minami_a@scphys.kyoto-u.ac.jp

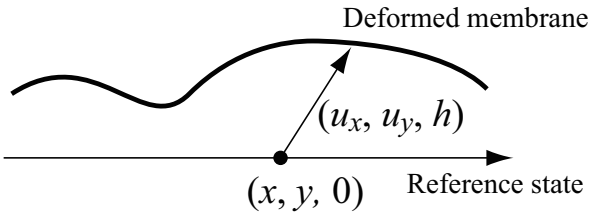

Fig. 1. Reference coordinate $(x, y, 0)$ and deviation vector (u_x, u_y, h).

2.1 Free energy functional

In this model, we consider fluid-like membranes, in which bending deformations and in-plane dilations are introduced to consider the buckling elasticity, and we do not consider in-plane shear deformations as in crystalline membranes [24]. We assume that the membrane is initially not deformed, and set this as a reference state. We set the z-axis of the Cartesian coordinate (x, y, z) perpendicular to the membrane. A displacement vector $(\boldsymbol{u}, h) = (u_x, u_y, h)$ is also introduced to describe elastic deformation of the membrane. The initial position $(x, y, 0)$ is moved to the position $\overrightarrow{r} = (x+u_x, y+u_y, h)$ (see Fig. 1). In this paper, we describe three-dimensional vectors by an over-arrow like $\overrightarrow{r}$, and describe two-dimensional vectors by bold italic characters like $\boldsymbol{u}$. In the following sections, a gradient operator ∇ is defined as the two-dimensional operator as $\nabla = (\nabla_x, \nabla_y)$.

The tangential vectors of the membrane along the xy-axes are written as

$$\overrightarrow{r_x} \equiv \frac{\partial \overrightarrow{r}}{\partial x} = \big(1 + \nabla_x u_x, \nabla_x u_y, h_x\big), \tag{1}$$

$$\overrightarrow{r_y} \equiv \frac{\partial \overrightarrow{r}}{\partial y} = \big(\nabla_y u_x, 1 + \nabla_y u_y, h_y\big), \tag{2}$$

where $h_\alpha \equiv \nabla_\alpha h$. In case of the fluid membranes, positions of molecules on the membranes are rearranged by in-plane shear deformations and elongations. The change of the geometry by the shear and the elongation and the shape of the domains are described by convective terms of hydrodynamics. Although it is quite interesting to analyze the dynamics of the rearrangement, we do not consider such hydrodynamic effects to avoid complexity. Thus, we assume no shear deformation ($\nabla_y u_x = \nabla_x u_y = 0$) and no elongation ($\nabla_x u_x - \nabla_y u_y = 0$) at each time. Only a dilation defined by $e \equiv \nabla \cdot \boldsymbol{u}$ has finite value. Consequently, we find $\nabla_x u_x = \nabla_y u_y = e/2$.

Here, we divide the displacement vector $\boldsymbol{u}$ into an applied deformation $\boldsymbol{u}^0 = (u_x^0, u_y^0)$ and its deviation $\delta\boldsymbol{u} = (\delta u_x, \delta u_y)$ as $\boldsymbol{u} = \boldsymbol{u}^0 + \delta\boldsymbol{u}$. Consequently, we also divide the dilation e into a uniform dilation $\bar{e}$ and its deviation δe as $e = \bar{e} + \delta e$. The meaning of $\bar{e}$ is the area fraction of the applied deformation with respect to the total area S. If the membrane is compressed ($\bar{e} < 0$), the membrane is buckled. Due to the high incompressibility of the fluid membrane, the area of the applied deformation $S_{\rm ex} \equiv -S\bar{e}$ escapes in the z-direction. Therefore, $S_{\rm ex}$ is thought of as the excess area.

We assume that the magnitude of $|\nabla\delta\boldsymbol{u}|$ is much smaller than that of $|\nabla\boldsymbol{u}^0|$ and $(\nabla h)^2$. We also assume that $|\delta\boldsymbol{u}^0|$ and $(\nabla h)^2$ are much smaller than 1. To sum up, in this model, we assume

$$|\nabla\delta\boldsymbol{u}| \ll \left|\nabla\boldsymbol{u}^0\right| \sim (\nabla h)^2 \ll 1. \tag{3}$$

By considering the assumptions mentioned above, the metric tensor of the deformed surface is written as

$$g_{\alpha\beta} = \overrightarrow{r_\alpha} \cdot \overrightarrow{r_\beta} = \begin{pmatrix} 1 + e + h_x^2 & h_x h_y \\ h_x h_y & 1 + e + h_y^2 \end{pmatrix}, \tag{4}$$

where $\alpha, \beta = x, y$. Its determinant g and inverse tensor $g^{\alpha\beta}$ are given by

$$g = \det(g_{\alpha\beta}) = 1 + 2e + (\nabla h)^2, \tag{5}$$

$$g^{\alpha\beta} = \frac{1}{g}\begin{pmatrix} 1 + e + h_y^2 & -h_x h_y \\ -h_x h_y & 1 + e + h_x^2 \end{pmatrix}. \tag{6}$$

Because we consider liquid-like membranes, the shear modulus μ is zero. Therefore, the two parts — the in-plane dilation $\sqrt{g} - 1$ and the mean curvature of the membrane $2H \approx -\nabla^2 h$ — can contribute to the elastic energy. Ignoring higher than third order of $\sqrt{g}$ and $\nabla^2 h$, we write the elastic energy as

$$\begin{aligned}\mathcal{F}_{\rm el} &= \int \sqrt{g}\mathrm{d}\boldsymbol{r}\left[\frac{\lambda}{2}\big(\sqrt{g} - 1\big)^2 + 2\kappa H^2\right] \\ &\approx \int \mathrm{d}\boldsymbol{r}\left[\frac{\lambda}{2}\left(e + \frac{1}{2}(\nabla h)^2\right)^2 + \frac{\kappa}{2}\big(\nabla^2 h\big)^2\right].\end{aligned} \tag{7}$$

Here κ is the bending coefficient, and λ is the elastic coefficient of the compression and expansion. Because most fluid membranes are highly incompressible, the energy scale of the coefficient λ is much larger than any other energy coefficients appearing in this theory. Thus, the contribution from the in-plane compression δe is not negligible in the term proportional to λ, although δe is order of magnitude smaller than the applied deformation $\bar{e}$. Furthermore, the time scale of the in-plane mode $\delta\boldsymbol{u}$ is much shorter than that of the off-plane mode h or the order parameter ϕ, and the sound of the in-plane mode propagates through the whole membrane instantaneously. Therefore, in the time scale of the phase separation and the buckling, the in-plane deformation $\boldsymbol{u}$ is in mechanical equilibrium. Then, we minimize the elastic energy with respect to $\boldsymbol{u}$ as

$$-\frac{\delta\mathcal{F}_{\rm el}}{\delta\boldsymbol{u}} \approx \lambda\nabla\left(\delta e + \frac{1}{2}(\nabla h)^2\right) = \boldsymbol{0}. \tag{8}$$

Remember that δe is the deviation from the average deformation $\bar{e}$, so the average of the strain deviation δe is $\langle\delta e\rangle = 0$. Here, we introduce the symbol $\langle a\rangle = \int \mathrm{d}\boldsymbol{r} a(\boldsymbol{r})/S$ representing the spatial average of a. Then, we can solve the above equation as

$$\delta e = -\frac{1}{2}\left[(\nabla h)^2 - \left\langle(\nabla h)^2\right\rangle\right], \tag{9}$$

where

$$\left\langle (\nabla h)^2 \right\rangle = \frac{1}{S}\int \mathrm{d}\boldsymbol{r}(\nabla h)^2. \tag{10}$$

The metric g is approximated by considering the assumption (3) as

$$g \approx 1 + 2\bar{e} + (\nabla h)^2, \tag{11}$$

and the elastic energy $\mathcal{F}_{\mathrm{el}}$ is rewritten as

$$\mathcal{F}_{\mathrm{el}} \approx \int \mathrm{d}\boldsymbol{r}\left[\frac{\lambda}{2}\left(\bar{e} + \frac{1}{2}\left\langle (\nabla h)^2 \right\rangle\right)^2 + \frac{\kappa}{2}\left(\nabla^2 h\right)^2\right]. \tag{12}$$

This result is consistent with Uchida's theory of buckling membranes [25]. If the applied dilation is negative ($\bar{e} < 0$), the solution $\nabla h = 0$ becomes unstable, and the membrane is in buckling. On the other hand, if the applied dilation is positive ($\bar{e} > 0$), the solution $\nabla h = 0$ is stable, and then the expansion with respect to ∇h until the second order is justified if $\nabla h \ll 1$. In this case, (12) is approximated as

$$\mathcal{F}_{\mathrm{el}} \approx \int \mathrm{d}\boldsymbol{r}\left[\frac{\Sigma}{2}(\nabla h)^2 + \frac{\kappa}{2}\left(\nabla^2 h\right)^2\right], \tag{13}$$

where Σ is the surface tension defined by $\Sigma = \lambda\bar{e} > 0$. Here we use the definition (10). This form is the same as the elastic energy used in reference [23]. Remember that our theory (12) includes the case $\Sigma < 0$.

In this paper, we do not consider the hydrodynamic interaction mediated by the solvent or the membrane. The component of both sides of the membrane is assumed to be the same, and the spontaneous curvature difference is zero. Then, in our model, we do not consider the bilinear coupling $\phi\nabla^2 h$ between the order parameter ϕ and the curvature $\nabla^2 h$ appearing in references [12–14]. We then write the free energy of the phase separation as follows:

$$\begin{aligned}\mathcal{F}_0 &= \int \sqrt{g}\mathrm{d}\boldsymbol{r}\left[f(\phi) + \frac{C}{2}\left(\nabla_{\mathrm{s}}\phi\right)^2\right] \\ &\approx \int \mathrm{d}\boldsymbol{r}\left[f(\phi) + \frac{C}{2}\left(\nabla_{\mathrm{s}}\phi\right)^2\right].\end{aligned} \tag{14}$$

Here, the first term of the integrand is the ϕ^4-theory

$$f(\phi) = \frac{r}{2}\phi^2 + \frac{u}{4}\phi^4. \tag{15}$$

The second term is the gradient energy evaluated on the deformed surface written by the metric tensor as [20]

$$\begin{aligned}\frac{C}{2}\left(\nabla_{\mathrm{s}}\phi\right)^2 &= \frac{C}{2}g^{\alpha\beta}\phi_\alpha\phi_\beta \\ &= \frac{C}{2}\left(\nabla\phi\right)^2 - \frac{C}{2g}\left[\bar{e}(\nabla\phi)^2 + (\nabla\phi\cdot\nabla h)^2\right],\end{aligned} \tag{16}$$

where $\phi_\alpha = \nabla_\alpha\phi$. Let us explain the meaning of this term. This term becomes minimum if ∇h and $\nabla\phi$ are parallel. From the buckling dynamics viewpoint, the bending deformation occurs near the interface between two components, and its direction is perpendicular to the interface. Consider the membrane and the interface as a soft ball and a string tied on the ball, respectively. If the ball is bound with the string, the surface is transformed into a vertical direction to the string line. This is analogous to the deformation of the membrane by the line tension (phase boundary). Therefore, the coupling between the surface and the composition in (16) is not unnatural. From the phase separation dynamics viewpoint, the length of the domain boundary favors the minimum route on the deformed surface.

The total free energy is written as

$$\mathcal{F} = \mathcal{F}_{\mathrm{el}} + \mathcal{F}_0. \tag{17}$$

We minimize this free energy by the relaxation method.

2.2 Dynamic equations

The dynamic equation of the deformation h is the over-damped form

$$\begin{aligned}\tau_h\frac{\partial h}{\partial t} &= -\frac{\delta\mathcal{F}}{\delta h} \\ &= \nabla^2\left[\lambda\left(\bar{e} + \frac{1}{2}\left\langle (\nabla h)^2\right\rangle\right) - \kappa\nabla^2\right]h \\ &-C\nabla\cdot\left[\frac{\nabla h\cdot\nabla\phi}{g}\nabla\phi - \frac{\bar{e}\left(\nabla\phi\right)^2 + \left(\nabla h\cdot\nabla\phi\right)^2}{g^2}\nabla h\right].\end{aligned} \tag{18}$$

This over-damped form is justified if the membrane is in the viscous liquid. In this equation, the spatial average $\left\langle (\nabla h)^2\right\rangle$ is included. This means that the local deformation of the membrane is affected by the global deformation. In other words, if the local area increases or decreases at some points, the local displacement $\delta\boldsymbol{u}$ propagates over the system to compensate the local area increase and decrease by the global area.

The dynamics of the phase separation is written by the Cahn-Hilliard form.

$$\begin{aligned}\tau_\phi\frac{\partial\phi}{\partial t} &= \nabla_{\mathrm{s}}^2\frac{\delta\mathcal{F}}{\delta\phi} \\ &\approx \nabla^2\left[f'(\phi) - C\nabla^2\phi + \nabla\cdot\frac{C}{g}\left(\bar{e}\nabla\phi + (\nabla h\cdot\nabla\phi)\nabla h\right)\right],\end{aligned} \tag{19}$$

where $f'(\phi) = r\phi + u\phi^3$, and we omit the applied deformation $\bar{e}$ and bending deformation ∇h in the first Laplacian.

3 Analysis

In all numerical analysis, we choose the following parameters. In the Cahn-Hilliard dynamics, we set $r = -1$, $u = 1$, and $C = 1$. The bending coefficient κ is set as $\kappa = 2$. We set the dilation coefficient λ as large as numerically possible, in order to reflect high incompressibility of membranes. In this simulation, we set $\lambda = 4000$. The time scale of the deformation h is in many cases shorter than that of the phase separation [14]. Thus, we choose $\tau_h = 0.1$ and

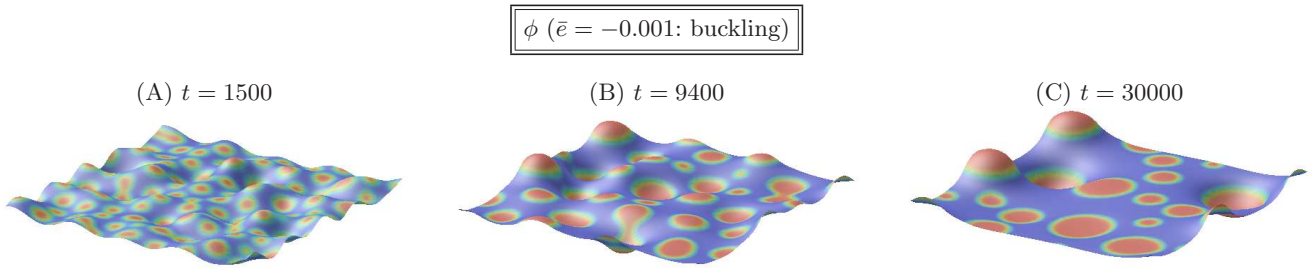

Fig. 2. (Colour on-line) Phase separation on a buckled membrane ($\bar{e} = -0.001 < 0$) with average composition $\langle\phi\rangle = -0.3$. Red and blue areas show $\phi > 0$ and $\phi < 0$, respectively. The height of the membrane is twice exaggerated.

$\tau_\phi = 1$. Because ϕ is conserved, we initially set average composition $\langle\phi\rangle$ as $\langle\phi\rangle = -0.3$ and $\langle\phi\rangle = 0$.

Related to the digitization method, we set the width of the spatial lattice $\Delta x = 1$, and the time step is discretized by $\Delta t = 0.01$. We use the Euler scheme under the periodic boundary condition in the xy plane. The number of the lattice along the x and y axes (N_x and N_y) are equally chosen as $N_x = N_y = 128$. As an initial condition, we put uniform random numbers with an amplitude 0.01 to $\boldsymbol{u}$ and h uniformly over the system.

3.1 Domain-induced budding

As can be seen in Figures 2, 3, and 4, the shape of the membrane is strongly affected by the presence of a little excess area. In Figures 2 and 3, we applied uniform compression $\bar{e} = -0.001$ to the membrane as an initial condition ($t = 0$). We started with the average composition $\langle\phi\rangle = -0.3$ and $\langle\phi\rangle = 0$ in Figures 2 and 3, respectively. In Figure 2 ($\langle\phi\rangle = -0.3$), the component $\phi > 0$ is minority, and then the region $\phi > 0$ forms droplet structures. In this case, the domain budding is observed at $t = 9400$ (see (B) in Fig. 2). The membrane is deformed at the domain boundary. The minority domains form caps and the majority domains become flat (see Fig. 2 (C)). However, we must note that all the domains not always have the same height. The height of the caps depends on the initial condition and parameters. In the critical composition case (Fig. 3), the components $\phi > 0$ and $\phi < 0$ are equally prepared. Then the domain structure is bicontiunous. Compared to the case of the critical composition case in Figure 3, the minor component which form droplets (red one in Fig. 2) draw excess area from the buckling membrane. Figure 4 shows the phase separation on the extended membrane ($\bar{e} = 0.001 > 0$). No excess area is present if the membrane is extended, and then we observe no budding domain. If the membrane is completely incompressible ($\lambda \to \infty$), budding domain never appears. Let us analyze the single-domain budding in this limit.

3.2 Single-domain case

In this section, we investigate the single-domain budding theoretically.

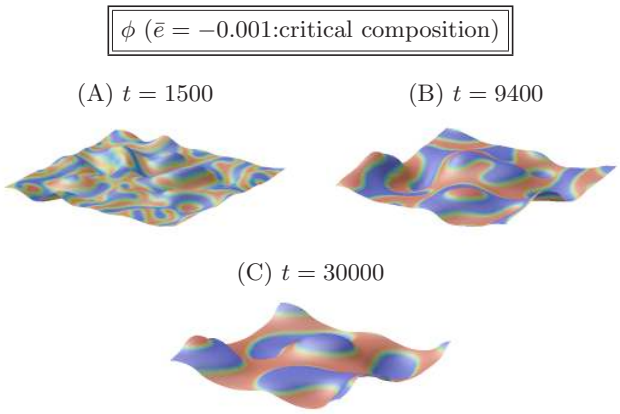

Fig. 3. (Colour on-line) Phase separation on a buckled membrane ($\bar{e} = -0.001 < 0$) with average composition $\langle\phi\rangle = 0$. Red and blue areas show $\phi > 0$ and $\phi < 0$, respectively. The height of the membrane is twice exaggerated.

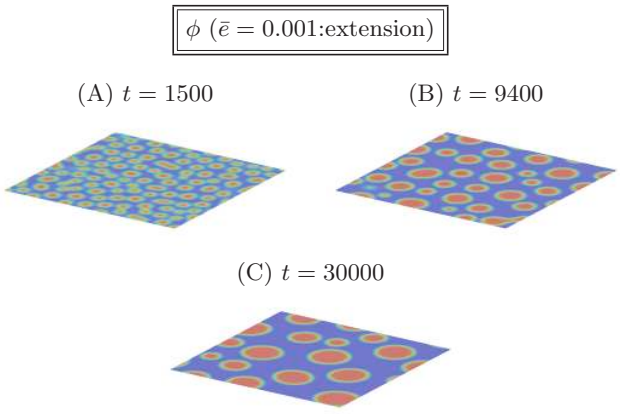

Fig. 4. (Colour on-line) Phase separation on a flat membrane ($\bar{e} = 0.001 > 0$) with average composition $\langle\phi\rangle = -0.3$. Red and blue areas show $\phi > 0$ and $\phi < 0$, respectively. The height of the membrane is twice exaggerated.

Assume that a circular domain with radius L is on a membrane with area S. The curvature radius and the curvature of the domain is R and $H = 1/R$, respectively. We define the neck radius of the budding domain N. Figure 5 shows the schematic picture of this situation. We calculate

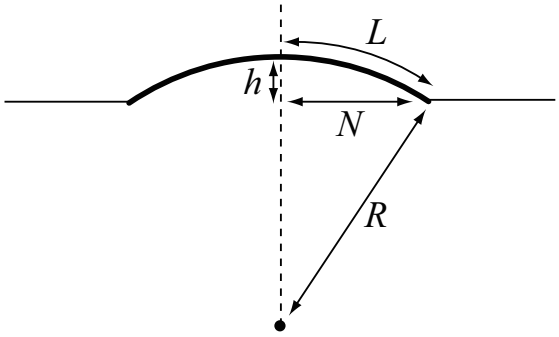

Fig. 5. Bending deformation starting from the domain boundary [26]. The thick line shows a circular domain on a membrane, which has curvature $H = 1/R$.

the elastic energy and the line energy, and minimize with respect to the curvature H.

From the geometrical consideration [26], we obtain a relation $N^2 = L^2(1 - (LH)^2/4)$. Then, the area increase ΔS is calculated as

$$\Delta S = \pi L^2 - \pi N^2 = \frac{\pi}{4}\left(L^2 H\right)^2. \tag{20}$$

The increase of the stretching energy $\Delta E_{\rm st}$ due to this increase is written as

$$\Delta E_{\rm st} = \frac{\lambda \bar{e}}{2}\Delta S + \frac{\lambda}{8S}(\Delta S)^2, \tag{21}$$

and the increase of the bending energy $\Delta E_{\rm bend}$ is written as

$$\Delta E_{\rm bend} = \int \mathrm{d}\boldsymbol{r}\frac{\kappa}{2}\left(\nabla^2 h\right)^2 \approx 2\pi\kappa(LH)^2. \tag{22}$$

The bending energies of the bulk and the boundary are of the order of L^2 and $L\xi$, respectively, where ξ is the thickness of the domain boundary. Then, the bending energy of the boundary is negligible if the domain size is much larger than the interface thickness. In this paper, we consider this case. The length of the domain boundary is changed by the budding, and the line tension decreases as

$$\Delta E_{\rm line} = 2\pi\sigma L - 2\pi\sigma N \approx -2\pi\sigma L(LH)^2, \tag{23}$$

where σ is the line tension of the domain boundary which is written as $\sigma \sim C(\Delta\phi)^2/\xi$, where $\Delta\phi$ is the order parameter difference between two domain, and ξ is the thickness of the domain boundary. Then, the total energy increment is $\Delta E = \Delta E_{\rm st} + \Delta E_{\rm line} + \Delta E_{\rm bend}$, and we minimize this with respect to the reduced curvature LH with large λ. Then, we obtain the budding height $h \approx L^2 H$ as

$$h \approx L^2 H = \sqrt{\frac{8S}{\pi}\left[-\bar{e} + \left(1 - \frac{\ell}{L}\right)\frac{2\sigma}{L\lambda}\right]}, \tag{24}$$

where $\ell = \kappa/\sigma$, and we use the relation $h \approx L^2 H$ when the domain is weakly budding. In most theories, completely incompressible condition or no incompressibility are considered. However, in real membranes, the membrane is more or less compressible, but this compressibility is very small.

If we apply completely incompressible condition $\lambda \to \infty$, the situation becomes different as

$$h = \left(\frac{-8\bar{e}S}{\pi}\right)^{1/2} = \left(\frac{8S_{\rm ex}}{\pi}\right)^{1/2}. \tag{25}$$

The height of the domain budding is completely governed by the excess area $S_{\rm ex}$. Therefore, without the excess area, the cap-shaped domains are never created if the membrane is completely incompressible.

Next, we check the consistency with the previous theory issued by Lipowsky [26]. When neither extension nor compression is applied ($\bar{e} = 0$), the above relation is rewritten as

$$h = \sqrt{\frac{8S}{\pi}\left(1 - \frac{\ell}{L}\right)\frac{2\sigma}{L\lambda}}. \tag{26}$$

If $L > \ell = \kappa/\sigma$, a small budding domain appears. As in reference [26], budding height is determined by the bending energy and the line tension, but the height of the budding domain is suppressed by the surface area constraint as mentioned above.

In real systems, the membrane can be compressed a little bit though it is highly incompressible. The height of the budding is not determined only by the line tension and the curvature energy like (24), or only by the buckling like (25). The height of the budding is determined both by the line tension and the excess area like (24). If the excess area $S_{\rm ex}$ is sufficient, the budding domain appears without satisfying the condition $L > \ell$.

In our analysis, we neglect the bending energy at the kink of the domain boundary. This approximation is justified in the limit of large line tension. By evaluating the kink bending energy

$$\Delta E_{\rm kink} \sim \kappa\left(\frac{h}{\xi L}\right)^2 \times \xi L = \kappa\frac{h^2}{\xi L}, \tag{27}$$

we compare the line tension energy $\Delta E_{\rm line}$ and $\Delta E_{\rm kink}$. The kink contribution is neglected if $\Delta E_{\rm kink}/\Delta E_{\rm line} \sim \kappa/\sigma\xi \ll 1$. Thus, the approximation is justified if $\xi \gg \kappa/\sigma = \ell$, or the limit of the large line tension.

3.3 Multiple domains and domain coalescence

In the single-domain case, the budding height is uniquely determined by the domain radius and the excess area. However, if there are two or more domains, domain height is not uniquely determined by the domain radius. As can be seen in Figure 2, domains with same radius have different budding height. If one domain buds highly, another domain cannot bud without further excess area. This is experimentally observed.

Figure 6 shows the growth law of the phase separation. We numerically defined the number of simulation lattice points on domain boundaries $N_{\rm B}$ as follows. If at least one of the nearest-neighbor lattice points has the opposite

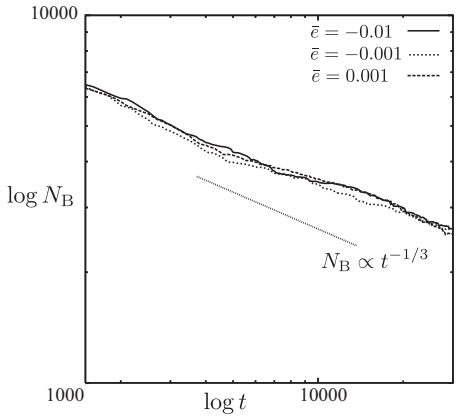

Fig. 6. Number of simulation lattice points on domain boundaries $N_{\rm B}$.

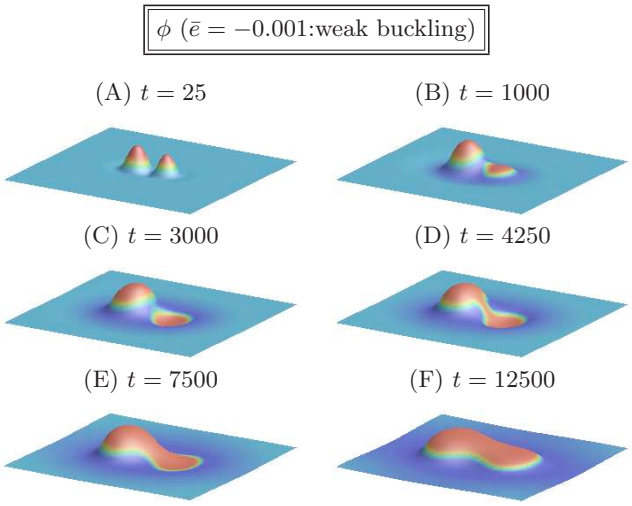

Fig. 7. (Colour on-line) Coalescence of two circular domains. The red region and the blue region represent regions $\phi > 0$ and $\phi < 0$, respectively. The height of the membrane is ten times exaggerated. As domains grow, one of these domains changes its budding direction, and then becomes single domain.

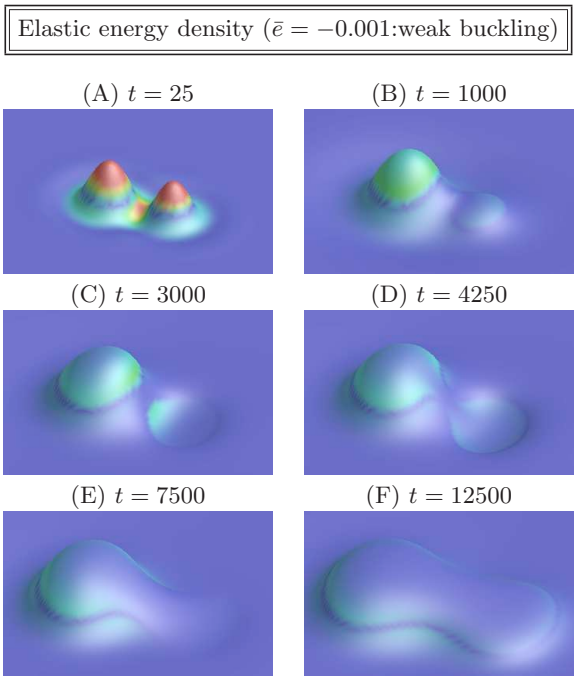

Fig. 8. (Colour on-line) Coalescence of two circular domains. The red region represents the region with elastic energy density larger than 0.004. The height of the membrane is ten times exaggerated. Larger elastic energy is localized between two domains, and this is released if one domain changes its direction.

sign, we count it as a point of domain boundaries [14]. As can be seen in Figure 6, the growth law of the phase separations on the membranes is not different regardless of being buckled ($\bar{e} < 0$) or expanded ($\bar{e} > 0$). In this sense, this model cannot describe the slow dynamics of the phase separation on vesicles [9].

In this model, domain growth occurs mainly by the evaporation or by the coalescence. According to the paper [9], the motion of domains is driven by thermal fluctuation (Brownian motion), and thus the growth is mainly due to the coalescence. Then, in this section, we examine the fusion of two domains on the buckling membranes.

We initially put two domains with height $h = 1$ and order parameter $\phi = 1.4$ in the environment $h = 0$ and $\phi = 0.6$, and check the coalescence of two domains. In our simulation, we put two domains with radius 5 at $x = 0.34N_x$ and $y = 0.5N_y$, and with radius 6.5 at $x = 0.58N_x$ and $y = 0.5N_y$, respectively. We initially applied weak compression $\bar{e} = -0.001$. This result is shown in Figure 7.

As the larger and smaller domains grow, the domains come closer. Interestingly, when the two domains coalesce, the smaller domain changes its budding direction to the opposite side of the membrane (see (B)-(D) in Fig. 7). After the coalescence, the smaller domain is drawn up to the direction of the larger cap (see (E) and (F) in Fig. 7). Figure 8 shows the elastic energy density on the surface. In (A) in Figure 8, the elastic energy density between two domains is larger than that of the other area outside the circular domains because the curvature between two domains becomes large when two domains become closer. This energy is released if one of the domain changes its direction to the opposite side (see (C) in Fig. 8) because the curvature between domains becomes smaller. Then two domains can be closer, and the coalescence is realized. This effect becomes prominent as the budding height becomes larger.

This result suggests the origin of a slow dynamics of phase separation on vesicles. In planar membranes, both sides of the membrane are equivalent. However, in vesicles, the two sides of the membrane are different. This is because the membranes of vesicles are closed, and then the two sides are apparently distinguishable. Furthermore, in many vesicles, the hydrostatic pressure inside and outside is different due to the osmotic pressure. By these reasons, the inside and the outside are not symmetric. In some cases, there is a spontaneous curvature difference between the two components [6,14], and the budding direction depends on the components. As can be seen in many

experimental snapshots [9,27], the directions of the budding in vesicles are basically limited to one direction. In such systems, the caps cannot change their direction, and then it might be difficult to release elastic energy between budding domains. Therefore, our results suggests that the domain coalescence and its slow dynamics are strongly affected by the closed nature of vesicles and the pressure difference between the inside and the outside.

4 Summary

In this paper, we have presented a mean-field description of budding phenomena on buckling membranes. To avoid complexity, we limited ourselves to an analysis of flat membranes.

Yanagisawa *et al.* suggested that the excess area of membranes plays an important role in the dynamics of phase separation on membranes. In order to take this effect into account, we have considered the buckling of the planer membrane and introduced the parameter representing the compression $\bar{e}$. The situations $\bar{e} < 0$ and $\bar{e} > 0$ correspond to the membrane with and without some excess area, respectively. Furthermore, we assumed that the membrane is slightly compressible and introduced the compressive elasticity modulus λ. This is different from most of the previous theoretical studies in which the membrane is perfectly incompressible. Note, however, that λ is very large compared with other parameters in the present study.

The main results are summarized as follows.

1. If the membranes are highly incompressible, the budding height is determined not only by the competition between the line tension and the bending energy, but also by the excess area arising from the buckling. For example in Figure 2, the phase separation accompanies the budding of domains if $\bar{e} < 0$. On the other hand, in the case $\bar{e} > 0$ shown in Figure 4, the budding does not occur although the phase separation proceeds similar to the case in which $\bar{e} < 0$.
2. When two caps with the same directions get closer, there is a large curvature energy between them (Fig. 8) because the curvature between them becomes larger as they get closer. Then, when they coalesce, one of the domains changes its direction to the opposite side (Fig. 7) in order to release the elastic energy between them.
3. The slow dynamics of the phase separation on vesicles is unfortunately not reproduced by our model. In vesicles, due to the osmotic pressure and the asymmetry of the inside and the outside, the directions of caps are usually limited to one direction. In such systems, the caps cannot change their budding direction when the domains become closer. Then the effective interaction between domains can be different from our results, and this may lead to the slow dynamics of the coarsening. In this paper, however, we have merely issued a suggestion related to the slow dynamics of the phase separation on vesicles. To provide quantitative analysis on the slow dynamics, it is important to extend our theory to spherical reference states like vesicles.

Additionally, we would like to mention the elastic theory of spherical shells. There are many theoretical publications related to the elasticity of spherical shells [28]. However, in the elastic theory of vesicles, many authors consider only the off-plane mode and its bending energy, and they neglect the in-plane degree of freedom and its elastic energy [29,30]. In their theories, the surface area constraint is introduced as a Lagrange multiplier. As mentioned in the literature [28,31], due to the geometrical constraint in closed shells, the shell cannot change its shape without changing its surface area. Even if the change of the surface area is small, we should not neglect the contribution from the stretching energy, because the elastic coefficient of the area change is large. A small number of authors [31,32] analyze the deformation and the buckling instability of shells with considering the in-plane mode.

In conclusion, we would like to mention the conceptual importance of the surface tension and the buckling phenomena in soft membranes. Compared to hard plates, bending operations are much easier than in-plane compressions in soft membranes because the typical bending energy is much smaller than the typical compression energy. Such energetic scale difference is introduced as the incompressibility of membranes in many theoretical analysis [14,22,29,30]. However, recently Komura *et al.* [23] theoretically reproduced the hexagonal and the stripe patterns on vesicles [21] by introducing the surface tension. Therefore, even though the soft membrane is highly incompressible, the in-plane compression and extension strongly affects the morphology of the soft membranes, and such energetic difference becomes greatly prominent if we buckle the membranes. We would like to emphasize that the buckling elasticity can be one of the important aspects of the softness of biological membranes.

We would like to thank T. Hamada, M. Yanagisawa, M. Imai, S. Komura and T. Ohta for valuable discussions on the experimental and theoretical points of view.

References

1. K. Simons, E. Ikonen, Nature **387**, 569 (1997).
2. S.L. Veatch, S.L. Keller, Phys. Rev. Lett. **89**, 268101 (2002).
3. C. Dietrich, L.A. Bagatolli, Z.N. Volovyk, N.L. Thompson, M. Levi, K. Jacobson, E. Gratton, Biophys. J. **80**, 1417 (2001).
4. A.V. Samsonov, I. Mihalyov, F.S. Cohen, Biophys. J. **81**, 1486 (2001).
5. S.L. Veatch, S.L. Keller. Biophys. J. **85**, 3074 (2003).
6. T. Baumgart, S.T. Hess, W.W. Webb, Nature **425**, 821 (2003).
7. S.L. Veatch, S.L. Keller, Phys. Rev. Lett. **94**, 148101 (2005).
8. D. Saeki, T. Hamada, K. Yoshikawa, J. Phys. Soc. Jpn. **75**, 013602 (2006).

9. M. Yanagisawa, M. Imai, S. Komura, T. Ohta, Biophys. J. **92**, 115 (2007).
10. S. Leibler, D. Andelman, J. Phys. (Paris) **48**, 2013 (1987).
11. F. Jülicher, R. Lipowsky, Phys. Rev. Lett. **70**, 2964 (1993).
12. T. Kawakatsu, D. Andelman, K. Kawasaki, T. Taniguchi, J. Phys. II **3**, 971 (1993).
13. T. Taniguchi, K. Kawasaki, D. Andelman, T. Kawakatsu, J. Phys. II **4**, 1333 (1994).
14. T. Taniguchi, Phys. Rev. Lett. **76**, 4444 (1996).
15. P.B.S. Kumar, G. Gompper, R. Lipowsky, Phys. Rev. Lett. **86**, 3911 (2001).
16. W.T. Góźdź, G. Gompper, Europhys. Lett. **55**, 587 (2001).
17. M. Laradji, P.B.S. Kumar, Phys. Rev. Lett. **93**, 198105 (2004).
18. M. Laradji, P.B.S. Kumar, J. Chem. Phys. **123**, 224902 (2005).
19. J.L. Harden, F.C. MacKintosh, P.D. Olmsted, Phys. Rev. E **72**, 011903 (2005).
20. Z.G. Wang, J. Chem. Phys. **99**, 4191 (1993).
21. S. Rozovsky, Y. Kaizuka, J.T. Groves, J. Am. Chem. Soc. **127**, 36 (2005).
22. J.G. Hu, R. Granek, J. Phys. II **6**, 999 (1996).
23. S. Komura, N. Shimokawa, D. Andelman, Langmuir **22**, 6771 (2006).
24. T. Kohyama, D.M. Kroll, G. Gompper, Phys. Rev. E **68**, 061905 (2003).
25. N. Uchida, Physica D **205**, 267 (2005).
26. R. Lipowsky, J. Phys. II **2**, 1825 (1992).
27. R. Lipowsky, R. Dimova, J. Phys.: Condens. Matter **15**, S31 (2003).
28. L.D. Landau, E.M. Lifshitz, *Theory of Elasticity* (Wiley, New York, 1970).
29. O. Zhong-can, W. Helfrich, Phys. Rev. Lett. **59**, 2486 (1987).
30. J.T. Jenkins, J. Math. Biol. **4**, 149 (1977).
31. H. Yoon, J.M. Deutsch, Phys. Rev. E **56**, 3412 (1997).
32. S. Komura, K. Tamura, T. Kato, Eur. Phys. J. E **18**, 343 (2005).